Modulation of release and pharmacokinetics from nanoscale lipid prodrugs of dexamethasone with variable linkage chemistry

Mujeeb Ur-Rehman, Franceline Reynaud, Sinda Lepetre, Sonia Abreu, Pierre Chaminade, Elias Fattal, Nicolas Tsapis

Modulation of release and pharmacokinetics from nanoscale lipid prodrugs of Dexamethasone with variable linkage chemistry

Mujeeb-ur-Rehman[a,b], Franceline Reynaud[a,c], Sinda Lepetre[a], Sonia Abreu[d], Pierre Chaminade[d], Elias Fattal[a*], Nicolas Tsapis[a*]

[a] Université Paris-Saclay, CNRS, Institut Galien Paris-Saclay, 91400 Orsay, France.
[b] L.E.J. Nanotechnology Center, H.E.J. Research Institute of Chemistry, International Center for Chemical and Biological Sciences, University of Karachi, Karachi-75270 , Pakistan.
[c] Université de Lorraine, CITHEFOR EA3452, Faculté de Pharmacie, 54000, Nancy, France.
[d] Université Paris-Saclay, Lipides : systèmes analytiques et biologiques, 91400 Orsay, France.

Corresponding authors :
Elias Fattal, elias.fattal@universite-paris-saclay.fr
Nicolas Tsapis, Nicolas.tsapis@universite-paris-saclay.fr

Graphical abstract

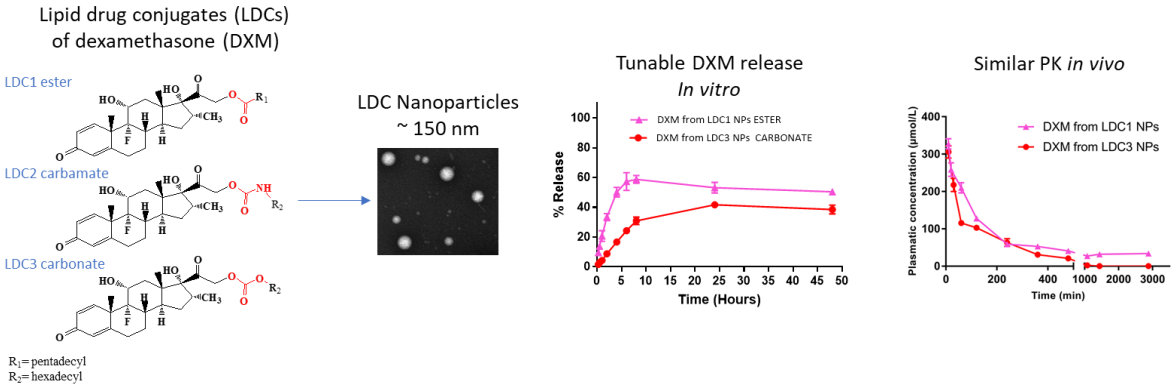

Abstract:
In an attempt to tune drug release and subsequent pharmacokinetics once administered intravenously, we have synthesized three lipid-drug conjugates (LDCs) of dexamethasone (DXM) each possessing a different lipid-drug chemical linkage: namely ester, carbamate and carbonate. These LDCs were thoroughly characterized before being turned into nanoscale particles by an emulsion-evaporation process using DSPE-PEG_{2000} (Distearoyl-sn-Glycero-3-Phosphoethanolamine-N-(methoxy(polyethylene glycol)-2000) as the only excipient. Spherical nanoparticles (NPs) of about 140-170 nm, with a negative zeta potential, were obtained for each LDC and exhibited good stability upon storage at 4 °C for 45 days with no recrystallization of LDCs observed. LDC encapsulation efficacy was above 95% for the three LDCs, leading to a LDC loading of about 90% and an equivalent DXM loading above 50%. Although the ester and carbonate NPs did not exhibit any toxicity up to an equivalent DXM concentration of 100 µg/mL, the carbamate LDC NPs appeared very toxic towards Raw264.7 macrophages and were discarded. Both ester and carbonate LDC NPs were shown to exert anti-inflammatory activity on LPS-activated macrophages. DXM release from LDC NPs in murine plasma was faster from ester than from carbonate NPs. Finally, pharmacokinetics and biodistribution were conducted, showing a lower exposure to DXM from carbonate LDC NPs than from ester LDC NPs, correlated with the slower DXM release from carbonate LDC NPs. These results outline the need for extended studies to find the best prodrug system for extended drug release.

1. Introduction:

Adrien Albert, in 1958, used the term “prodrug” for the first time to indicate a chemical entity that is therapeutically inactive, used to temporarily modify the physicochemical behavior of a drug to improve its bioavailability[1,2]. In practice, the prodrug term usually indicates a covalent link between a drug and an additional chemical moiety that leads to a pharmacologically inactive molecule. Prodrugs can then be chemically or enzymatically transformed to recover the parent active drug and exert their pharmacological effects[3–5]. Designing a prodrug offers numerous advantages such as increased solubility, improved bioavailability, enhanced stability, better selectivity, and reduced side effects depending on the moiety linked to the drug[6].
Glucocorticoids (GCs), are known anti-inflammatory and immunosuppressive drugs that suffer from severe side effects, particularly in the case of long-term therapy[7,8]. These side effects are mainly due to their undesirable distribution as well as the existence of glucocorticoid receptors (GR) throughout the body[9,10]. Encapsulation of GCs into different nanocarriers was considered to modulate their pharmacokinetics and distribution and reduce their side effect by facilitating their accumulation at inflamed sites using liposomes[11–14], micelles[15], polymeric nanoparticles[16] or hydrophilic and amphiphilic polymer prodrugs[17–22]. Our group recently developed a novel strategy to formulate hydrophobic lipid drug conjugates of glucocorticoids directly into PEGylated nanoparticles (NPs) using DSPE-PEG_{2000} (Distearoyl-sn-Glycero-3-Phosphoethanolamine-N-(methoxy(polyethylene glycol)-2000) as the only excipient[23–25]. In particular, Dexamethasone palmitate, an LDC of dexamethasone (DXM) was successfully formulated into NPs exhibiting prolonged circulation and an accumulation into inflamed joints of arthritic mice[23,24].
In a strategy to modulate the parent dexamethasone pharmacokinetics and biodistribution, we propose here to go beyond the ester linkage between dexamethasone and the palmitate moiety. Three different LDCs/prodrugs of dexamethasone were synthesized by varying the chemical linkage with the lipidic moiety: ester, carbamate and carbonate to yield LDC1 (dexamethasone palmitate,

ester linkage), LDC2 (Hexadecyl isocyano dexamethasone, carbamate linkage) and LDC3 (Hexadecyl formoyl dexamethasone, carbonate linkage). The ester linkage is reported to be the more labile, followed by the carbonate one and then carbamate one [26,27]. After thorough characterization, LDCs were formulated by emulsion-evaporation into NPs using DSPE-PEG_{2000} as an excipient. LDC NPs were characterized in terms of size, polydispersity, and zeta potential. Their stability upon storage was evaluated. After quantifying LDC loading by HPLC, NP cytotoxicity and anti-inflammatory effect were assessed on RAW264.7 macrophages. Drug release from LDC NPs was measured after incubation with murine plasma. Finally, LDC NPs were administered intravenously to healthy mice to evaluate their impact on dexamethasone pharmacokinetics and biodistribution.

2. Materials and Methods

2.1 Materials

Palmitoyl chloride, dexamethasone, hexadecyl isocyanate, anhydrous dichloromethane, and triethyl amine were purchased from Sigma Aldrich (France). Hexadecyl chloroformate was obtained from Tokyo Chemical Industry, Co. LT (Japan). LDC1, LDC2, and LDC3 were synthesized as described below. DSPE-PEG_{2000} was obtained from Avanti Polar Lipids, Inc. (USA). MilliQ reference system from Millipore (France) was used to purify water. Chloroform HPLC-grade (Carlo Erba Reagents, France), methanol, and acetonitrile HPLC-grade (VWR Chemicals, France) were used. NMR spectra were recorded on Bruker Avance-NMR (300, and 400 MHz) spectrometers in $CDCl_3$. ESI-MS of compounds were measured on Thermofisher Scientific (LTQ, ion trap, H-ESI II). All experiments were performed in amber vials due to the photosensitivity of dexamethasone palmitate[28]

2.2 Prodrugs synthesis and characterization

Dexamethasone was used as the active pharmaceutical ingredient (API) in this study. LDCs **1**, **2**, and **3** were synthesized from the API in the lab. as follows. Dexamethasone (784 mg) was dissolved in anhydrous dichloromethane (100 mL) in a round bottom flask (250 mL). Palmitoyl chloride (600 µL for LDC **1**) or Hexadecylisocyanate (620 µL for LDC **2**) or Hexadecylchloroformate (655 µL for LDC **3**) was added to the dexamethasone solution and stirred until the solution became clear. Triethyl amine (306 µL) was then added into the clear solution dropwise while stirring. The reaction mixture was left under an argon atmosphere (round bottom flask), overnight stirring at 30 °C for 24 hours. Finally, column chromatography (silica gel) was carried out to purify LDC **1, 2,** and **3**.

LDC 1: White amorphous powder; NMR data, see **Supporting Information** Table-TS1; positive ESI-MS m/z 631.5 $[M+1]^+$, 653.5 $[M+Na]^+$.

LDC 2: White amorphous powder; NMR data, see **Supporting Information** Table-TS1; positive ESI-MS m/z 660.5 $[M+1]^+$, 682.5 $[M+Na]^+$.

LDC 3: White amorphous powder; NMR data, see **Supporting Information** Table-TS1; positive ESI-MS m/z 661.5 $[M+1]^+$, 683.5 $[M+Na]^+$.

*2.3 LDC (**1**,**2**,**3**) Nanoparticle Formulation*

All three LDC **1**,**2**,**3** were formulated into nanoparticles by an emulsion-evaporation method as described by Lorscheider et al.[24]. Briefly, 25 mg of LDC1 or LDC2, or LDC3 and 12.5 mg of DSPE-PEG_{2000} were dissolved in 1 mL of chloroform. The organic phase was then injected into the 5 mL of prechilled water at 4 °C, using a syringe (Inject, B. Braun, France) and a 20Gx$2^{3/4}$ needle. At first, the mixture was pre-emulsified by vortexing (30 seconds) and then placed under ultra-sonication at an

amplitude of 40% (300 W using a VibraCell sonicator, Fisher Scientific, France) in an ice bath (2 minutes). The organic solvent was then evaporated under reduced pressure using a rotary evaporator (Buchi, France) to yield a final suspension volume of 5 mL. Finally, nanoparticle suspension was stored either at 4 °C or room temperature, protected from light in amber vials.

2.4 Size, polydispersity index, and zeta potential measurement

Zetasizer nano-ZS (Malvern Instrument, UK) was used to measure the size, polydispersity index, and zeta potential of the prepared nanoparticles, based on dynamic light scattering (DLS) principle (size, PDI) or laser doppler velocimetry (zeta potential). Size measurements were recorded at an angle of 173° (25°C) after 20-fold dilution in water. For zeta potential measurement, the 20-fold dilution was performed in NaCl (1 mM, pH 6.8-6.9) at 25°C.

2.5 Transmission electron microscopy (TEM)

Nanoparticles were analyzed by TEM at I2BC (CNRS, Gif-sur-Yvette, France). 5 µL of nanoparticle formulation containing 2.5 mg/mL of LDC1, or LDC2 or LDC3 were placed for 40 seconds on formvar-coated copper grids (400 mesh). The extra suspension was removed from the copper grid by using Whatman filter paper. A drop of the negative staining agent, uranyl acetate (2% w/w) was used and the excess was removed. Samples were imaged a few hours after grid preparation. The micrographic observation of the nanoparticles was performed on a JEOL 1400 microscope at an acceleration voltage of 80 kV. Finally, images were acquired using an Orius Camera (Gatan Inc, USA).

2.6 Encapsulation efficiency (EE) and Drug loading (DL)

Encapsulation efficiency was calculated indirectly by dosing free LDCs and DSPE-PEG_{2000} in the supernatant of NP suspension after ultracentrifugation. Ultracentrifugation was carried out at 40 000 rpm (=109 760g) for 4h at 4 °C (Beckman Coulter Optima LE-80K ultracentrifuge, 70-1Ti rotor), to separate free LDCs **1**, **2** and **3** and DSPE-PEG_{2000} from nanoparticles. The supernatant was instantly separated and freeze-dried (Alpha 1-2 LD Plus, Bioblock, France). Lyophilizates were dissolved in the mobile phase to give appropriate concentrations within the calibration curve range for HPLC analysis. Quantification of dexamethasone encapsulated LDCs **1**, **2**, **3** and DSPE-PEG_{2000} was performed by using HPLC coupled to an evaporative light-scattering detector (ELSD) and a UV detector. DSPE-PEG_{2000} can only be detected through ELSD detector, whereas. LDCs **1**, **2**, and **3** could be detected with both detectors. ELSD detection was performed according to the following conditions; a nebulization temperature (35 °C) and an evaporation temperature (45 °C), and UV detection was performed at 240 nm wavelength. The column (symmetry Shield TM RP18, 5µm, 250x4.6 mm; Waters, France) was eluted with mobile phase (100 % methanol with 0.104 % triethyl amine and 0.043 % acetic acid) at room temperature for 6 minutes at 1 mL/min flow rate. A volume of 50 µL of each sample (supernatant, pellet of suspension) was injected and the run time was set at 6 minutes. Retention times were 5.1, 5.2, and 5.0 minutes for LDCs **1**, **2**, and **3**, respectively, while the retention time for DSPE-PEG_{2000} was 3.9 minutes. To acquire calibration curves for quantification, the concentration ranges were 5-500 µg/mL for LDCs **1**, **2**, and **3** and 10-500 µg/mL for DSPE-PEG_{2000}, respectively. UV calibration curve of LDCs **1**, **2**, and **3** followed a linear model, y = 52.976x-201.31, R^2 = 0.9998., y = 51.576+171.54, R^2 = 0.9998., and y = 56.616+167.48, R^2 = 0.9999 for LDCs **1**, **2**, and **3**, respectively. Similarly, ELSD detection calibration curves also followed the linear model, equation, and correlation coefficient were, y = 20.822x-18.727, R^2 = 0.9975 for DSPE-PEG_{2000}. Encapsulation efficiency (EE) was determined as the percentage of LDCs **1**, **2**, and **3** or DSPE-PEG_{2000} encapsulated

related to the initial amount used for the preparation of LDCs **1**, **2**, and **3**-NPs. Similarly, prodrug loading values correspond to the proportion of LDCs **1**, **2**, and **3** encapsulated in mass compared to the total mass of the LDCs **1**, **2**, and **3**-NPs (including DSPE-PEG_{2000}). The equivalent dexamethasone loading was then calculated.

2.7 Drug release in plasma

LDC **1** and **3**-NPs prepared (5/2.5 mg/mL, LDC **1** or **3**/DSPE-PEG_{2000}) as described above were diluted in water to yield a final concentration of 260 and 210 µg/mL of dexamethasone, respectively. To quantify LDC **1** and **3** and dexamethasone in plasma, an extraction method was developed; 180 µL of plasma samples were introduced into Eppendorf and 20 µL of the LDC **1** and **3**-NPs introduced, vortexed for 10-15 seconds, and incubated at 37°C for different times. Afterward, 400 µL of acetonitrile was added into Eppendorf followed by vortexing vigorously for 30 seconds to precipitate out enzymes/proteins present in plasma. Then, centrifugation was performed at 13 400 rpm (20075 g) for 10 minutes (ST16R centrifuge, rotor TX-400, Thermo Scientific, France). The supernatant organic phase was collected and hence LDC **1**, **3,** and dexamethasone were quantified by HPLC-UV.

A Waters chromatographic module (717 Plus autosampler) equipped with a Waters 2487 dual λ absorbance UV detector and Waters 1525 binary HPLC pump were used. Breeze was used as software. Detection analysis was carried out at 240 nm. A conventional RP-18 column, SymmetryShieldTM (5 µm, 250x4.6 mm; Waters, Saint-Quentin-en-Yvelines, France) was used at room temperature. Eluent A consisted of 95:5 water:acetonitrile, and eluent B of 100% acetonitrile. The gradient mobile phase system used is shown in Table-TS**2 (Supporting information)**. The flow rate was 1 mL/min, the injection volume was 50 µL and the run time was 40 min. Retention times were 24, 27, and 8.5 minutes for LDCs **1**,**3** and dexamethasone, respectively. To acquire a calibration curve for quantification, the concentration ranges were 1-100 µg/mL for LDCs **1**, **3** (LOQ=1 µg/mL), and 0.5-100 µg/mL for dexamethasone (LOQ=0.5 µg/mL), respectively. UV calibration curve of LDCs **1**, **3**, and dexamethasone followed linear models, y = 20836x-12758, R^2 = 0.9972, y = 16958x+27926, R^2 = 0.9914., and y = 48952x-7838.5, R^2 = 0.9970 for LDCs **1** ,**3** and dexamethasone, respectively.

2.8 Cell culture

All *in vitro* cell culture assays were performed on murine macrophage cell line RAW 264.7 obtained from ATCC (USA), cultured in DMEM (Dulbecco`s Modified Eagle`s Medium) culture medium supplemented with 10% fetal bovine serum (FBS), penicillin G (10 000 unit/mL) and streptomycin (10 mg/mL), maintained in a humidified incubator at 37°C supplied with 5% CO_2. Cells were split twice per week at 1/10 ratio using a scraper to detach them and were used between passages 3 to 15.

2.9 Cell viability

The effect of formulations on cell viability was studied on the RAW 264.7 cell line using the MTT (3-[4,5-dimethylthiazol-2-yl]-3,5-diphenyl tetrazolium bromide) colorimetric assay[29]. Cells were seeded in 96-well plates at a density of 8 x 10^3 cells/well (24h Test) and 4 x 10^3 cells/well (48h Test) and incubated until 80% confluence. Then, the medium was replaced by fresh medium with *Escherichia coli* lipopolysaccharides (LPS) at 1.0 µg/mL to activate macrophages, and plates were incubated for 3 h. Afterwards, LDC **1**, **2,** and **3**-NPs were added at the final concentration between 2,0 and 500 µg/mL (eq DXM), dexamethasone disodium phosphate (DSP), solubilized in water, and then diluted in the culture medium to reach the same concentration of dexamethasone as nanoprodrugs was used as a control. Culture medium was used as negative control and LDC **1**, **2,** and

3-NPs alone in culture medium, without cells, were also tested to check their potential interference with the MTT assay. After 24 h or 48 h of incubation, 20 µL of 5 mg/mL yellow tetrazolium MTT solution was added to each well and incubated for another hour. The MTT is reduced by metabolically active cells to form the purple formazan crystals. After the formation of the crystals, the medium was discarded and replaced by 200 µL of DMSO to dissolve crystals and the absorbance was measured at 570 nm. The percentage of viable cells was calculated as the absorbance ratio between treated cells and untreated control cells. All measurements were performed in triplicate.

2.10 Cytokine release

The anti-inflammatory effect of LDC **1** and **3**-NPs was determined by activating RAW 264.7 cells with LPS. For the cytokine quantification, cells were seeded in 24-well plates at a cell density of $4x10^4$ cells/well in a culture medium and were incubated for 48 hours until 80% confluency. Then, the medium was replaced by fresh medium alone or fresh medium with LPS at 1.0 µg/mL, and plates were incubated for another 3 hours. Afterward, LDC **1** and **3**-NPs (100 and 104 µg/mL, respectively) and DSP (82 µg/mL) in a culture medium to reach the same equivalent concentration of dexamethasone. Culture medium alone was used as the negative control and LPS 1.0 µg/mL as the positive control. After 12, 24, and 48 hours of incubation with the treatments, cell supernatants were collected and frozen at -20°C until analysis was performed. Cells were detached and counted. Mouse inflammatory cytokines TNFα, MCP-1, IL-10, and IL-6 were quantified using a Cytometric Beads Array (CBA) detection kit (BD Biosciences, USA). In each test tube, 50 µL of mouse inflammation capture bead suspension was added, completed with either 50 µL of standards solution (20 - 5 000 pg/mL) or 50 µL of supernatant samples. 50 µL of phycoerythrin (PE) detection reagent was added to each tube and incubation for 2 h at room temperature was performed. Samples were washed with 1 mL wash buffer provided in the kit and tubes were centrifuged (200 g, 5 min) to recover the pellet. Then, 300 µL of wash buffer was added to resuspend the pellet and samples were quantified with the BD Accuri C6 Cytometer (BD Biosciences, USA). Cytokine secretions were analyzed with the FACP Array™ Software and were obtained as pg/mL concentrations. All measurements were performed in triplicate.

2.11 In vivo studies

In vivo experimental procedures using DBA/1OlaHsd mice were approved by ethical committee No. 026 and by the French Ministry of Education and Research (accepted protocol no. 2842-2015110914248481_v5). The number of animals was determined according to the power analysis method[30]. DBA/1OlaHsd male mice, aged 9-12 weeks, were purchased from Envigo (U.K.) and left for 1 week after shipping for adaptation before starting experiments. Mice were kept in a separate animal room under climate-controlled conditions with a 12 hours light/dark cycle, housed in polystyrene cages containing wood shavings, and fed standard rodent chow and water ad libitum. Mouse colonies were screened and determined to be pathogen-free.

2.11.1 Pharmacokinetics and Biodistribution

First, LDC**3** NPs were diluted in phosphate-buffered saline (PBS) to obtain a final concentration of 2.62 mg/mL of LDC**3** which corresponds to an equivalent of 1.55 mg/mL DXM. DBA/1OlaHsd male mice aged 10-12 weeks were anesthetized with Isoflorane (3.5 % v/v, for 2 min) and then 12 mg/kg (eq. DXM), an intermediate dose in the range found in the literature for efficacy in mice (1-60 mg/kg)[31], of LDC3 NPs were administered by retro-orbital injection[32]. 10 pharmacokinetics time

points were selected with 5 mice per time point. Blood sampling was achieved by terminal cardiac puncture using a 25G needle while mice were previously deeply anesthetized with Isoflorane (3.5 % v/v, for 5 min). Plasma was separated in a mini centrifuge (Eppendorf Minispin®, France) at 10000 rpm (7000 g), and subsequently frozen and stored at -80°C. For each time point, after a cardiac puncture, the liver, spleen, kidneys, and lungs were removed and stored at -80°C. The quantification of LDC3 and DXM in samples was determined by chromatography-tandem mass spectrometry (LC-MS/MS).

To quantify LDC3 and DXM in plasma, an extraction process was developed. First, 100 µL of plasma samples was introduced into centrifugation tubes, and 100 µL of internal standard (IS) mixture, testosterone decanoate (TestD) for LDC**3** and budesonide (BUD) for DXM, both at 4 µg/mL in acetonitrile were added and vortexed for 30 s. Then, 3 mL of a 9/1 chloroform/methanol (v/v) mixture was added, and tubes were vortexed vigorously for 3 min to precipitate proteins. Centrifugation was performed at 3500 rpm (1690 g) for 30 min (ST16R centrifuge, rotor TX-400, Thermo Scientific, France). The supernatant organic phase was recovered and evaporated using an evaporator under nitrogen gas flow (Sample Concentrator, Stuart, U.K.). Dried samples were dissolved into 200 µL of acetonitrile, and LDC**3** or DXM was quantified by LC-MS/MS.

To quantify LDC3, and DXM in organs, the liver, spleen, kidneys, and lungs were separately homogenized in PBS using a micro-pestle coupled with a turbine at 2000 rpm during the time needed to obtain a liquid preparation, approximately 5 min. LDC**3**/DXM were extracted from the homogenate using the same method as plasma extraction described above, beginning with 100 µg of homogenate for the liver and kidneys, 25 µg for the spleen and lungs completed up to 100 µg with MilliQ water. Then, 100 µL of IS mixture (Budesonide and TestD at 150 ng/mL) was added and vortex for 30 s, followed by the addition of 3 mL of 9/1 chloroform/methanol (v/v), vortexed for 3 min, and centrifuged in the same conditions as above. The organic phase was evaporated, and 200 µL of acetonitrile was added and mixed for 1.5 min. This final sample was analyzed by LC-MS/MS method.

2.11.2 LDC3 and DXM Quantification by LC-MS/MS method (for in vivo assays)

LDC3 and DXM after *in vivo* assays were quantified in plasma and in organs (Liver, spleen, kidneys, and lungs) by LC-MS/MS method. Chromatography was performed on a security guard cartridge (Eclipse XDB-C8, Narrow-Bore Guard Column with 5 µm particles and 2.1 x 12.5 mm, Agilent, USA) The mobile phase was a linear gradient of 40-100 % (v/v) 0.1 % formic acid in acetonitrile over 14 minutes followed by isocratic elution with 100 % acetonitrile for 11 minutes, and the pump flow rate was 0.3 µL/min. The aqueous solvent was 0.1 % formic acid. The LC-MS/MS system consisted of a triple quadrupole Quattro Ultima Waters equipped with an electrospray source coupled to an HPLC Ultimate 3000 Thermoscientific and an automatic injector WPS3000PL. The mass spectrometer was operated in the positive/ion mode. Ions were analyzed by multiple reactions monitoring (MRM). Transition ions were m/z 393.48/122.67 for DXM, m/z 641.55/399.37 for LCD3, m/z 413.33/323.21 for Budesonide (IS of DXM) and m/z 443.56/156.3 for TestD (IS of LDC3). A volume of 5 µL of samples was injected and analyzed for 25 min. Retention times were 4.3 min and 10.4 min for DXM and LCD3, respectively. Budesonide and TestD at 30 ng/mL were used as internal standards, with retention times 5.2 min and 13.9 min, respectively. The LC-MS methods were validated. The selectivity was confirmed for LDC3 and DXM. Calibration curves were linear, respectively in the range 1-500 ng/mL for LCD3 (LOQ=10 ng/mL), $R^2 = 0.9985$, $y = 113.5x + 497.8$, and for DXM (LOQ=10 ng/mL) $R^2 = 0.9984$, $y = 2147x - 26184$. Finally the repeatability was confirmed with CV=0.654 % and 0.586% for LDC3 and DXM, respectively.

2.12 Statistical analysis

Results were reported as the mean standard error of the mean (SEM). Statistical analysis was performed using GraphPad Prism 7.0 software.

3. Results and Discussion

3.1 LDC synthesis and characterization

Scheme-**1** shows the synthesis of the three LDCs. Nucleophilic addition/elimination reaction was carried out in anhydrous dichloromethane (DCM) between palmitoyl chloride and dexamethasone resulting in the formation of ester linkage in LDC **1**. Excess HCl produced during the reaction was quenched by adding triethyl amine (TEA) as a base. Carbamate linkage in LDC **2** was constructed by reacting hexadecyl isocyanate with dexamethasone in DCM (TEA, base). Similarly, carbonate linkage in LDC **3** by reacting hexadecyl chloroformate with dexamethasone in DCM (TEA, base). Synthesis yields of 63, 62, and 65% for LDCs **1**, **2**, and **3** were obtained, respectively.

LDC **1** was obtained as a white amorphous solid. The molecular weight of LDC **1** was confirmed from the ESI-MS, which exhibited an $[M+Na]^+$ peak at *m/z* 653.4, corresponding to $C_{38}H_{59}FO_6$+Na, ^{1}H-NMR, and the broad-band decoupled ^{13}C-NMR spectrum. The ^{13}C-NMR spectrum exhibited resonances for 38 carbons. The ^{1}H-, and ^{13}C-NMR spectra (Supporting Information **Table TS1**) showed characteristic resonances for four methyl groups [δ_H/δ_C 1.05 (s)/ 16.7 (CH_3-18); 1.54 (s)/23.1 (CH_3-19); 0.91 (s)/14.8 (CH_3-22); 0.88 (s)/ 14.3 (CH_3-16'), one oxygenated methylene [δ_H/δ_C 4.87 d/68.3 (HO-CH_2-21)], one oxygenated methin [δ_H/δ_C 4.38 m /72.5 (HO-CH-11)], one oxygenated tertiary carbon [δ_C 91.2 (HO-C-17)], one fluorinated tertiary carbon [δ_C 99.4 (FC-9)], one ketone group [δ_C 205.0 (C-20)], one ester group [δ_C 173.9 (C-1')], and an α,β-unsaturated ketone group [δ_C 186.7 (C-3)]. Heteronuclear Multiple Bond Correlation (HMBC) of H_2-21 (δ_H 4.87) with C-1' (δ_C 173.9), indicated the formation of ester linkage (**Supporting Information S1**).

Likewise, LDC **2** was obtained as a white amorphous solid. The molecular weight of LDC **2** was confirmed from the ESI-MS, which exhibited an $[M+Na]^+$ peak at *m/z* 682.5, corresponding to $C_{39}H_{62}FNO_6$ + Na, ^{1}H-NMR, and the broad-band decoupled ^{13}C-NMR spectrum. The ^{13}C-NMR spectrum exhibited resonances for 39 carbons. The ^{1}H-, and ^{13}C-NMR spectra (Supporting Information **Table TS1**) showed characteristic resonances for four methyl groups [δ_H/δ_C 1.06 (s)/ 16.7 (CH_3-18); 1.54 (s)/23.1 (CH_3-19); 0.90 (s)/14.8 (CH_3-22); 0.88(s)/14.3 (CH_3-18'), one oxygenated methylene [δ_H/δ_C 4.82 d/68.4 (HO-CH_2-21)], one oxygenated methin [δ_H/δ_C 4.37 m/72.5 (HO-CH-11)], one oxygenated tertiary carbon [δ_C 91.2 (C-17)], one fluorinated tertiary carbon [δ_C 99.5 (FC-9)], one ketone group [δ_C 206.4 (C-20)], one carbamate group [δ_C 156.1 (C-1')], and an α,β-unsaturated ketone group [δ_C 186.7 (C-3)]. HMBC correlations of H_2-21 (δ_H 4.82) with C-1' (δ_C 156.1), indicated the formation of carbamate linkage (**Supporting Information S1**).

Similarly, LDC **3** was obtained as a white amorphous solid. The molecular weight of prodrug **3** was confirmed from the ESI-MS, which exhibited an $[M+Na]^+$ peak at *m/z* 683.5, corresponding to $C_{39}H_{61}FO_7$+ Na, ^{1}H-NMR, and the broad-band decoupled ^{13}C-NMR spectrum. The ^{13}C-NMR spectrum exhibited resonances for 39 carbons. The ^{1}H-, and ^{13}C-NMR spectra (Supporting Information **Table TS1**) showed characteristic resonances for four methyl groups [δ_H/δ_C 1.06 (s)/16.1 (CH_3-18); 1.54 (s)/23.1 (CH_3-19); 0.92 (s)/14.8 (CH_3-22); 0.88 (s)/14.3 (CH_3-18'), one oxygenated methylene [δ_H/δ_C 4.90 d/70.8 (HO-CH_2-21)], one oxygenated methin [δ_H/δ_C 4.36 m /72.1 (HO-CH-11)], one oxygenated tertiary carbon [δ_C 91.1 (HO-C-17)], one fluorinated tertiary carbon [δ_C 99.4 (FC-9)], one ketone group [δ_C 204.7 (C-20)], one carbonate group [δ_C 155.4 (C-1')], and an α,β-unsaturated ketone group [δ_C

186.7 (C-3)]. HMBC correlations of H_2-21 (δ_H 4.90) with C-1' (δ_C 155.4), indicated the formation of carbonate linkage (**Supporting Information S1**).

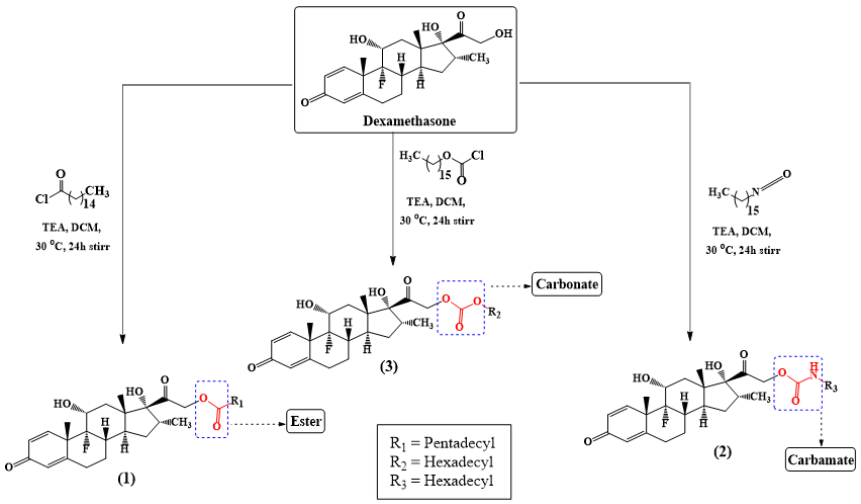

Scheme 1: Synthesis of Dexamethasone lipid drug conjugates LDCs 1 (ester), 2 (carbamate) and 3 (carbonate)

3.2 Formulation of LDCs in NPs

The emulsion-evaporation process was used to formulate LDC **1**, **2,** and **3**-NPs using DSPE-PEG_{2000} as an excipient. This process led to the formation of rather monodisperse spherical nanoparticles, as shown by TEM images (Figure 1) with hydrodynamic diameters of 170 nm, 150 nm, and 140 nm, respectively, PDIs around 0.2 and zeta potentials around -45 mV (Figure 2).

After formulation of LDCs **1**, **2,** and **3** NPs, their size, polydispersity index (PdI), and zeta potential were followed for 45 days at room temperature and 4 °C. LDCs **1**, **2,** and **3**-NPs stored at 4 °C proved to be stable in terms of size, and PdI. Under room temperature storage, size, and PdI started to increase after 20 days for LDC1, and after 45 days for LDCs 2 and 3 where a precipitate could be observed. The zeta potential of all LDC NPs exhibited a slight decrease over time from -45 down to -55 mV. This decrease might arise from a slight desorption of DSPE-PEG_{2000} over time. The precipitation is probably due to the Ostwald ripening of dexamethasone prodrugs/LDCs as observed before at room temperature with LDC1 due to crystal growth[24,28]. However, NPs of the three LDCs prepared by the emulsion-evaporation method present long-term stability at 4 °C, and do not require purification or freeze-drying.

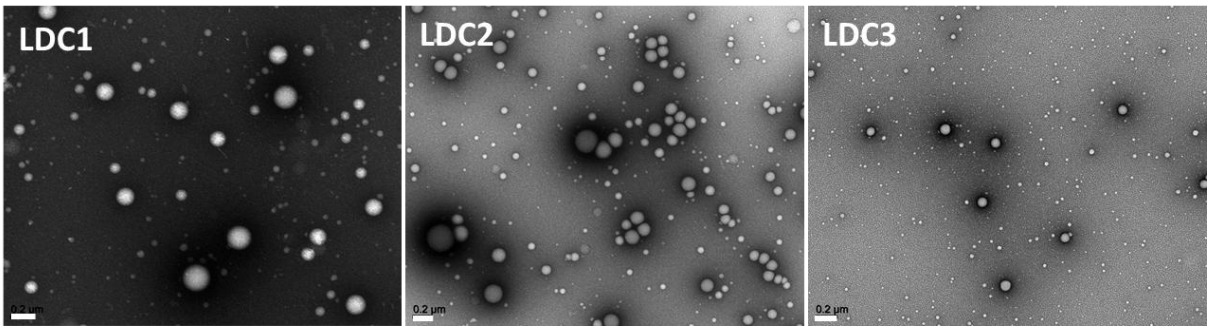

Figure 1: TEM micrographs of LDC **1**-NPs, LDC **2**-NPs and LDC **3**-NPs prepared by emulsion-evaporation, after negative staining. The scale bars represent 200 nm.

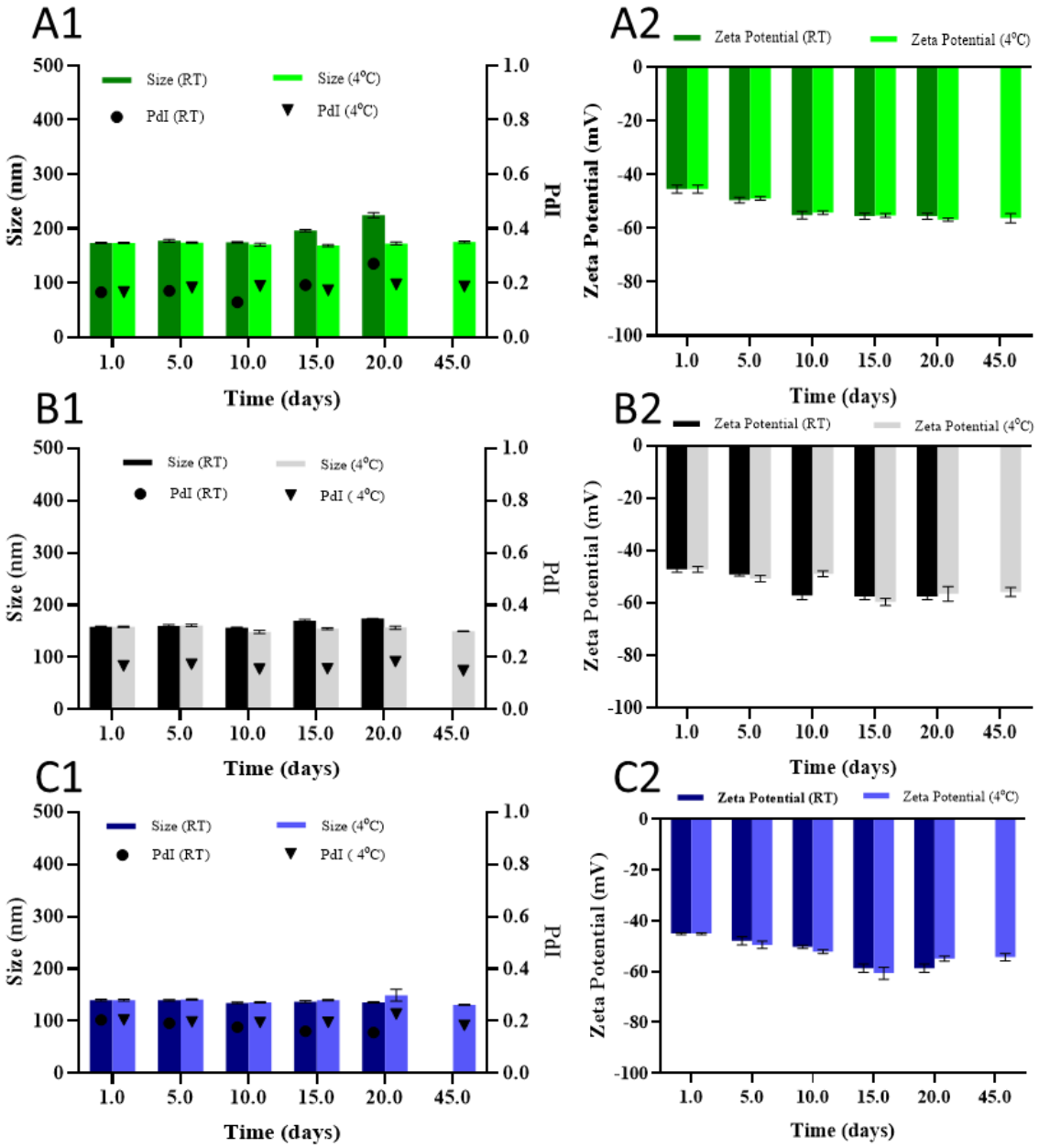

Figure 2: Hydrodynamic diameter (d_H) and PdI of LDC **1 (A1)**, **2 (B1)** and **3** NPs (**C1**), at room temperature (RT) or 4 °C over time. Zeta potential (mV) of LDC **1 (A2), 2 (B2),** and **3** NPs **(C2)**, at room temperature (RT) or 4 °C over time.

3.3 LDC encapsulation efficiency and LDC and drug loading

During NP preparation, DSPE-PEG_{2000} is expected to associate strongly with LDCs **1**, **2,** and **3** thanks to hydrophobic interactions between the distearoyl chains of DSPE-PEG_{2000} and the lipidic chains of LDCs [24]. However, DSPE-PEG_{2000} could also be present as micelles in the final suspension. A simple method of HPLC-ELSD-UV that can separate and detect both components in a single injection on the same chromatogram was developed. After separation by ultracentrifugation, non-encapsulated dexamethasone, LDC, and DSPE-PEG_{2000} in the supernatant were quantified and their amount in NPs was calculated indirectly. We observed that the formulation process led to 55, 30, and 35%

encapsulation of the initial amount DSPE-PEG$_{2000}$ in LDCs **1-**, **2-** and **3-**NPs, respectively (Figure 3). By contrast, 98, 97 and 98% of the initial amount of LDCs **1**, **2** and **3** were encapsulated in NPs (Figure 3). Considering the amounts of encapsulated compounds in NPs, the LDC loading, and corresponding active drug dexamethasone loading were calculated: LDC loading in NPs was around 90 % and the equivalent dexamethasone loading was of 56% (0.56mg/mg), 55% (0.55mg/mg) and 53% (0.53mg/mg) for LDC1 (ester), 2 (carbamate), and 3 (carbonate), respectively (Figure 3). The formulation process based on chemical linkage allows to reach rather high prodrug and drug loadings. Indeed physical encapsulation leads to drug loadings around 10-20 % at maximum[33], hydrophilic polymer prodrugs to drug loadings from 1% to 33 % at best for [18–20] and up to 50% for amphiphilic polymer conjugates of glucocortocoids [21,22]. Our LDC NP are definitely in the upper range of DXM loading[34].

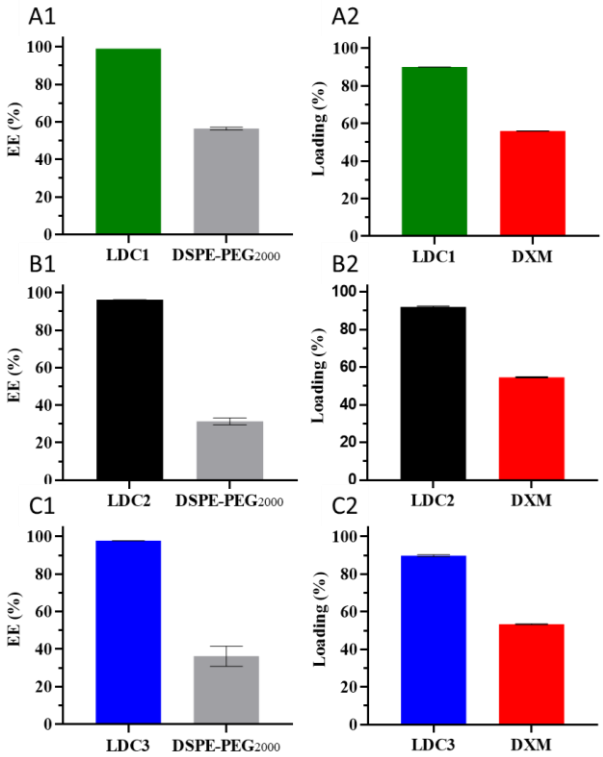

Figure 3: Encapsulation efficiency of LDC**1** (ester, green, A1), LDC**2** (carbamate, black, B1), LDC**3** (carbonate, blue, C1) and DSPE-PEG$_{2000}$ (grey) in prodrug nanoparticles, respectively. Prodrug and drug loadings corresponding to LDC**1** (green, A2), LDC**2** (black, B2), LDC**3** (blue, C2), and equivalent DXM loading (red) in prodrug nanoparticles.

3.4 Cell Viability

Before evaluating the ability of LDC NPs to exert an anti-inflammatory effect on activated macrophages, the potential cell toxicity of LDC **1-**, **2-,** and **3**-NPs was investigated by MTT assay on RAW 264.7 murine macrophages. A range of nanoprodrugs concentrations from 2,0 to 500 µg/mL (eq. DXM) was evaluated and compared to soluble dexamethasone (DSP) as a control. According to ISO guidelines for the MTT assay, potential cytotoxicity is defined when cell viability decreases below 70% of the control [35]. LDC **1-**, **3**-NPs, and DSP exhibited a very similar cytotoxicity profile. After 24 hours of incubation (**Figure 4-A**), these formulations and DSP did not induce a reduction of cell viability below an equivalent DXM concentration of 120 µg/mL. On the other hand, the results for LDC **2**-NPs showed that carbamate linkage led to pronounced cytotoxicity even at doses as low as 3.9

µg/mL(eq DXM). After 48 hours of incubation, the LDC **1** and **3** NPs and DSP clearly showed no cytotoxicity up to (eq. DXM) up to 62.5 µg/mL (**Figure-4-B**). One cannot see any significant differences between LDC **1** and **3**-NPs or DSP. Our results are in agreement with previous data demonstrating a relative safety of DXM versus RAW 264.7 murine macrophages [40]. The toxicity of carbamate LDC NPs should be investigated in more detail to identify the metabolites responsible for the decrease in cell viability. Given the results obtained on cells, LDC 2-NPs were discarded for further experiments. Since we observed an absence of cytotoxicity up to 120 µg/mL (eq. DXM) for LDC1 and LDC3 NPs, the inhibition of inflammatory cytokines (TNFα, MCP-1, IL-10 and IL-6) release was evaluated at 100 µg/mL (eq. DXM).

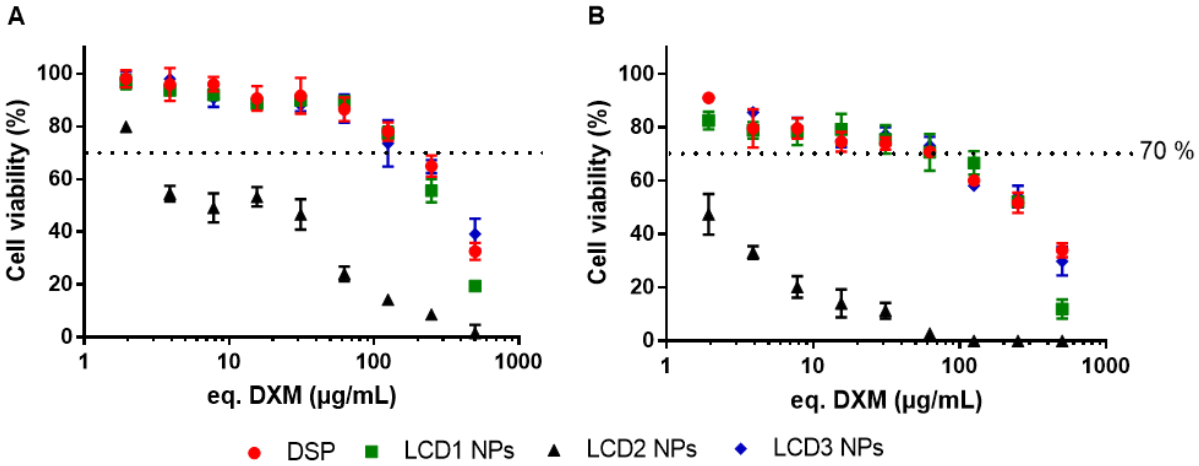

Figure 4: Raw 264.7 murine macrophages viability after 24 hours (A) and 48 hours (B) exposure to DSP solution (red circles), LCD 1-NPs (green squares), LCD 2-NPs (black triangles), LCD 3-NPs (blue diamonds) at different concentrations. Concentrations are expressed as equivalent DXM.

3.5 In vitro cytokine release

The release of pro-inflammatory cytokines (TNF-α, MCP-1, IL-10, and IL-6) by LPS-activated Raw 264.7 murine macrophages was quantified after their exposure to 100 µg/mL (eq. DXM) of LDC 1- and 3-NPs after 12, 24 and 48 hours incubation (**Figure 5**). DSP was used as a control. One can notice that dexamethasone nanoprodrugs LDC-NPs led to a reduction of cytokines secretion although to a different extent. TNF-α was significantly inhibited by LCD1-NPs after 12 hours of treatment, while LCD 3-NPS showed less efficacy to reduce the secretion of this cytokine, even after 48 hours of incubation (Figure 5-A). By contrast, MCP-1 was significantly reduced by both, LDC1 and LDC3 NPs after 48h but much less with LCD-3-NPS ($p<0.0001$) (**Figure 5-B**). The same profiles were observed for IL-6. These results probably arise from different DXM release kinetics from the NPs.

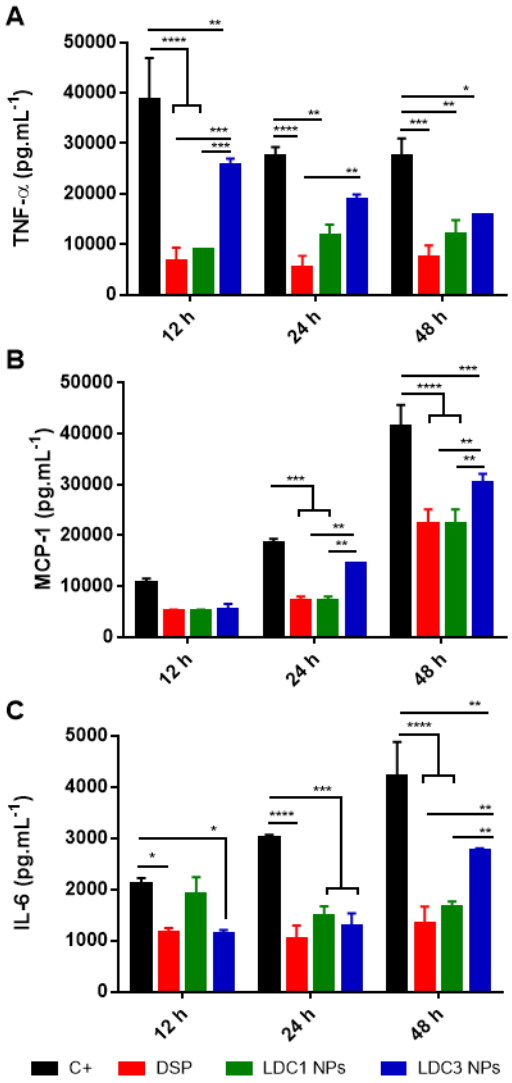

Figure 5: Quantification of cytokines TNF-α (A), MCP-1(B), and IL-6 (C) release from Raw 264.7 murine macrophages activated with LPS 1.0 µg/mL (C+, black) after treatment with 100 µg/mL (eq DXM) of DSP (red), LCD1 NPs (ester, green) and LCD3 NPs (carbonate, blue) as a function of time 12, 14 and 48 hours. Results are represented as mean ± SD (n = 3). Statistical analysis was performed with two-way ANOVA followed by Tukey's multiple comparisons tests (n = 6). ns = not significant, *p<0.1, **p<0.01, ***p<0.001, ****p<0.0001.

3.6 Drug release in plasma

To better understand cytokine release, LDC1 and LDC**3** NPs were incubated with murine plasma and the release of free DXM was monitored by HPLC method along with the decrease of LDC concentration over time. The release profiles showed that about LDC1 concentration decreased faster than LDC3 concentration reaching about 10% or 40% of the initial value at 6 h, respectively. Concurrently, DXM is released faster and to a greater extent (60%) from LDC1 NPs than for LDC3 NPs where a plateau of around 40% of DXM is reached after 24 h incubation. DXM release from LDC NPs is likely due to hydrolysis mediated by esterases present in plasma (**Figure 6**), before reaching a plateau. As expected, the ester linkage degrades faster than the carbonate one[36,37].The reason for which DXM is not totally released is unclear but this might result from partial degradation of dexamethasone or from metabolites formation as reported recently[38] as LDC1 and LDC3

concentration reaches zero over the course of 24 h. These results also allow to explain cytokines data. Indeed, as DXM is released faster form ester NPs than from carbonate NPs, cytokine secretion is inhibited to a higher extent by LDC1 ester NPs than by LDC3 carbonate NPs.

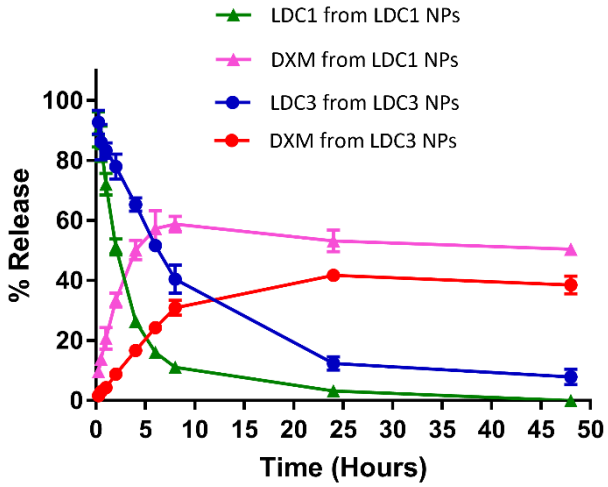

Figure 6: Dexamethasone (DXM) and nanoprodrugs (LDC**1** and LDC**3**) release profile in murine plasma. DXM release from LDC**1** NPs (ester, pink triangle) and LDC**3** NPs (carbonate, red circle), LCD**1** from LDC**1** NPs (ester, green triangle) and LCD**3** from LDC**3** NPs (carbonate, blue square)

3.7 Pharmacokinetics and Biodistribution

To obtain a better understanding of the behavior of LDC**3** NPs after intravenous injection, the pharmacokinetics and biodistribution of LDC3 and DXM were performed using the PK solver plugin from Excel (**Figure 7**). For the sake of clarity and comparison, plasmatic concentrations of LDC3 and DXM arising from LDC3 hydrolysis were compared with LDC1 and DXM resulting from LDC1 hydrolysis measured during previous experiments[24]. In these previous experiments from our group, LDC1 and DXM resulting from LDC1 hydrolysis were compared with the marketed soluble form of dexamethasone sodium phosphate. It was shown that ten minutes after injection, DXM from dexamethasone sodium phosphate was already at 10% of the injected dose proving it fast elimination from the blood stream [24]. This fast elimination of the soluble form was correlated to a quick accumulation in the liver [24].

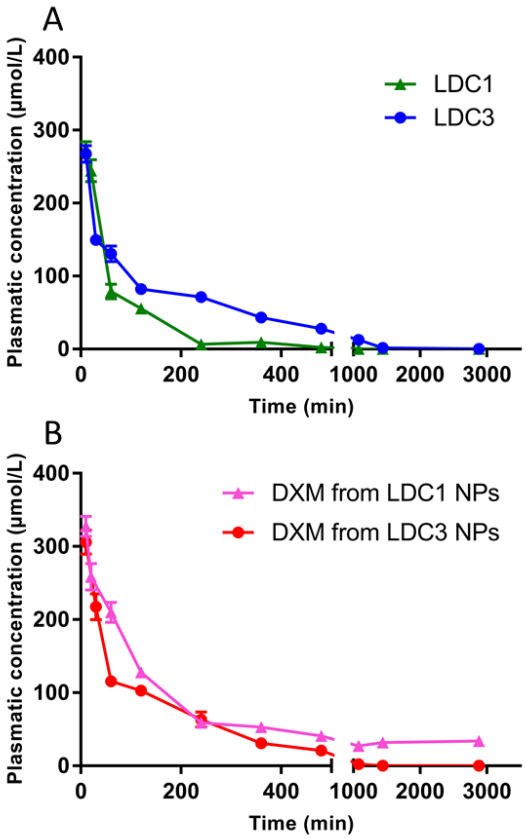

C

Pharmacokinetic parameters	DXM from LDC3 NPs
$T_{1/2}$ (min)	189
T_{max} (min)	10
C_{max} (µmol/L)	305
C_0(µmol/L)	362.9
$AUC_{0-\infty}$ (µmol*min/L)	44837
MRT (min)	203
Clearance (L/min)	$0.59x10^{-6}$
VD (L)	0.0161

Figure 7: (A) Pharmacokinetics of LDC1 (ester, green triangles, from [24]) and LDC3 (carbonate, blue circles) expressed as molar plasmatic concentration. (B) Plasma concentration of DXM from LDC1 NPs (ester, pink triangles, from [24].) and from LCD**3 NPS** (carbonate, red circles) Male DBA/1 healthy mice received an injection of 12 mg/kg (eq. DXM). Results are presented as mean ± SEM (n = 5). (C) Pharmacokinetic parameters of DXM from LDC3 NPs.

As for in vitro incubation with murine plasma, LDC1 plasmatic concentration decreases faster than LDC3 concentration due to the higher lability of the ester linkage over the carbonate linkage [26,36,37]. After 8 h almost no LDC1 could be detected in plasma whereas LDC3 was detectable until 18 h after injection (Figure 7A). After intravenous injection of NPs, DXM from LDC3 NPs was eliminated slightly faster than DXM from LDC1 NPs (Figure 7B)., The main pharmacokinetics

parameters of DXM from LDC3 NPs were calculated according to a noncompartmental model (**Figure 7C**). One can first notice that T_{max}, C_{max} and C_0 are in the same range for both prodrug NPs. The main differences reside in the exposure to the free DXM that is lower for LDC3 NPs than for LDC1 NPs. The area under the curve ($AUC_{0-\infty}$) of DXM from LDC**3** NPs was 44837 µmol*min/L 2.8 times lower than from LDC1 NPS (DXP-NPs) (126400 µmol*min/L, [24]). The $T_{1/2}$ and MRT are also shorter for LDC3 NPs than for LDC1 NPs 189 min and 203 min versus 971 min and 1967 min. Volume of distribution (Vd) values reveal that DXM from LDC**3** NPs (0.0161 L versus 0.0065 L for LDC**1** NPs) was more quickly distributed in the organs. LDC**3** acts as a prodrug, encapsulated into NPs, and seems to be hydrolyzed to release free DXM in the blood circulation. Even if DXM is released more slowly from LDC3 NPs than from LDC1 NPs, since once released DXM elimination is similar, the balance between release and elimination leads to a lower exposure to DXM for LDC3 NPs. Although surprising in first instance, this result is in good agreement with data obtained with polymer prodrugs of paclitaxel where the paclitaxel was released too slowly from the carbonate prodrug, leading finally to a lower exposure to the free drug than the one obtained with the ester prodrug[37].

Figure **8** presents the biodistribution of LDC**3** and DXM from LDC3 in liver, spleen, kidneys, and lungs. First, very small quantities of DXM or LDC3, lower than 1%, were detected in the lungs, proving NPs are small enough to circulate in the small capillaries. Among the four organs, the liver presents the highest accumulation of DXM from NPs with up to 20 % of the injected dose 120 min after injection, followed by a slow decrease until 18 h, due to the intrinsic accumulation of DXM in the [39], as observed previously with ester LDC NPs [24]. One can also notice a small accumulation of LDC3 NPs in the spleen, below 5% of injected dose, a common feature of PEGylated NPs [24,40]. On the other hand DXM concentration in spleen is very low. Part of LDC3 NPs are eliminated by urinary excretion as shown by concentration found in the kidney, most probably the smallest NPs. Overall, Pharmacokinetics results are correlated with biodistribution evaluation. In the liver, the small amounts of LDC**3** detected indicate that PEGylation of NPs allows a reduction of their opsonization, helping them escape from the immune system recognition in the bloodstream[41].

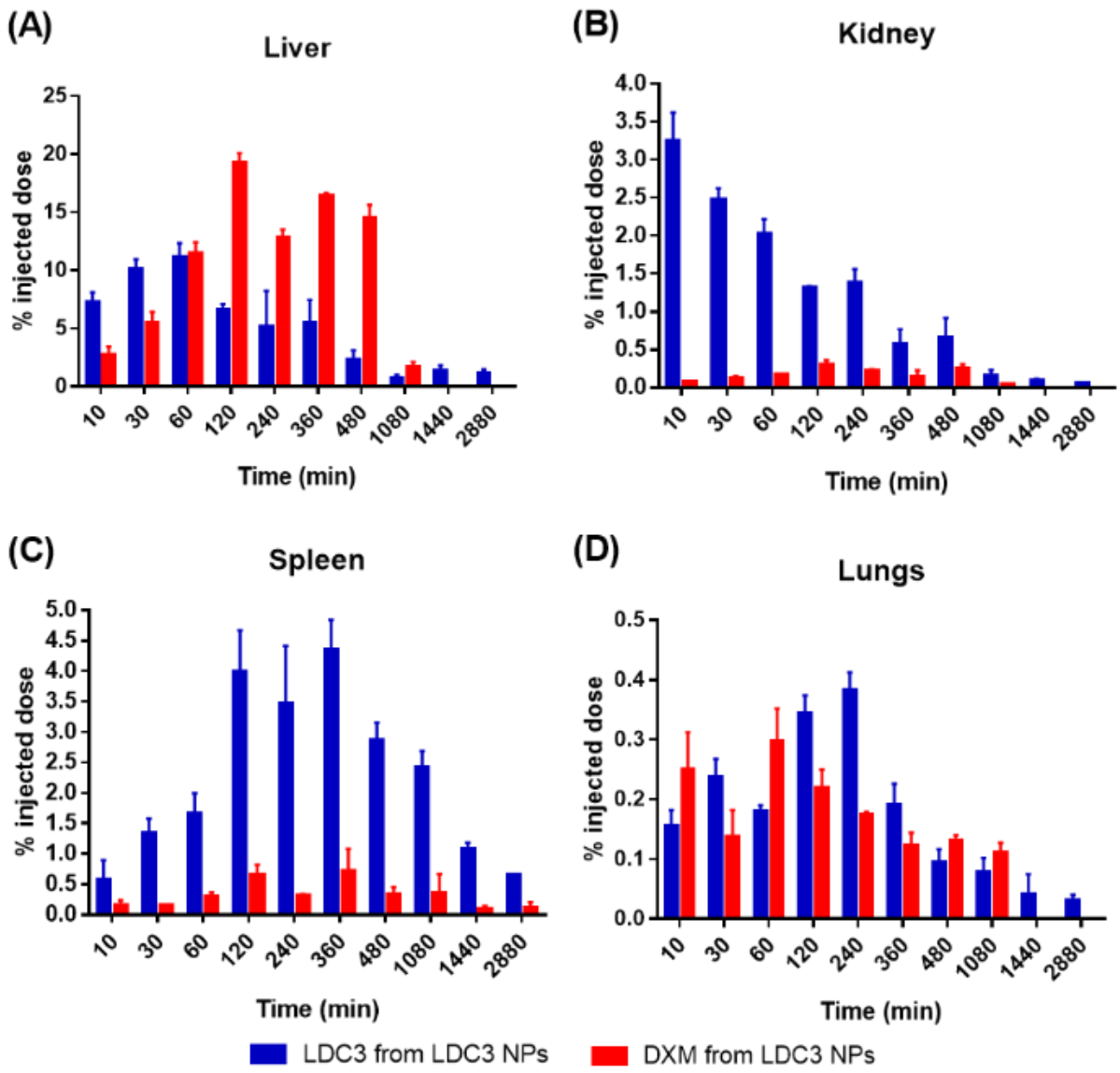

Figure 8: Biodistribution of LCD **3**-NPs (LCD **3** in blue and DXM in red) after of 12 mg/kg (eq. DXM) injected dose on male DBA/1 healthy mice. Quantification was performed in (A) liver, (B) kidney, (C) spleen and (D) lungs. Results are presented as mean ± SEM (n = 5)

4 Conclusion

We have successfully synthesized LDCs of DXM with either ester, carbamate or carbonate linkage. These LDCs were easily formulated into spherical NPs of 140-170 nm using DSPE-PEG_{2000} as the only excipient by an emulsion-evaporation process. NPs exhibited a good stability upon storage at 4 °C during 45 days. LDC encapsulation efficacy was above 95% for the three LDCs, leading to a LDC loading of about 90% and an equivalent DXM loading above 50%. Although the ester and carbonate NPs did not exhibit any toxicity up to an equivalent DXM concentration of 100 µg/mL, the carbamate LDC NPs appeared very toxic to RAW264.7 macrophages. The origin of the observed toxicity of the carbamate LDC should be further investigated by identifying if either the LDC itself or its metabolites are involved. Both ester and carbonate LDC NPs were shown to exert an anti-inflammatory activity on LPS-activated macrophages. The higher inhibition of pro-inflammatory cytokines observed with the ester LDC NPs is well correlated with the faster DXM release in murine plasma than from carbonate NPs. Finally, pharmacokinetics and biodistribution were conducted, showing a surprisingly

lower exposure to DXM from carbonate LDC NPs than from ester LDC NPs. This lower exposure arises from a too slow release of DXM from carbonate LDC NPs leading to the fast elimination of the drug from the blood stream. These results outline the need of extended studies to find the best prodrug system for extended drug exposure.

Acknowledgments

The authors would like to acknowledge the organizers of Pakistan-France PERIDOT Research Mobility Program (No.PhaseVII-1/PERIDOT.R&D/HEC/2021), jointly implemented by the Higher Education Commission, Pakistan, and Ministry of Foreign Affairs & International Development (MAEDI) and the Ministry of Higher Education and Research (MESRI), France. The present work has benefited from the core facilities of Imagerie-Gif, (http://www.i2bc.paris-saclay.fr), member of IBiSA (http://www.ibisa.net), supported by "France-BioImaging" (ANR-10-INBS-04-01), and the Labex "Saclay Plant Science" (ANR-11-IDEX-0003-02). Authors would like to thank S. Denis for her help with cell culture, A. Solgadi and B Prost (SAMM, IPSIT, Université Paris-Saclay) for LC-MS experiments and N. Ibrahim for fruitful discussions.

References:

[1] A. Albert, Chemical aspects of selective toxicity, Nature. 182 (1958) 421–423. doi:10.1038/182421A0.

[2] N. Liu, J. Tu, Y. Huang, W. Yang, Q. Wang, Z. Li, C. Sheng, Target- and prodrug-based design for fungal diseases and cancer-associated fungal infections, Adv. Drug Deliv. Rev. 197 (2023) 114819. doi:10.1016/J.ADDR.2023.114819.

[3] V.J. Stella, R.T. Borchardt, M.J. Hageman, R. Oliyai, H. Maag, J.W. Tilley, Prodrugs, Springer New York, New York, NY, 2007. doi:10.1007/978-0-387-49785-3.

[4] P. Banerjee, G. Amidon, Design of Prodrugs, in: Bundgaard H (Ed.), Elsevier, New York, 1985: pp. 93–133.

[5] C.E. Müller, Prodrug approaches for enhancing the bioavailability of drugs with low solubility, Chem. Biodivers. 6 (2009) 2071–2083. doi:10.1002/CBDV.200900114.

[6] Y. Yang, H. Aloysius, D. Inoyama, Y. Chen, L. Hu, Review, Acta Pharm. Sin. B. 3 (2011) 143–159. doi:10.1016/J.APSB.2011.08.001.

[7] A.K. McDonough, J.R. Curtis, K.G. Saag, The epidemiology of glucocorticoid-associated adverse events., Curr. Opin. Rheumatol. 20 (2008) 131–137.

[8] K.G. Saag, R. Koehnke, J.R. Caldwell, R. Brasington, L.F. Burmeister, B. Zimmerman, J. a Kohler, D.E. Furst, Low dose long-term corticosteroid therapy in rheumatoid arthritis: an analysis of serious adverse events., Am. J. Med. 96 (1994) 115–23.

[9] N.C. Nicolaides, Z. Galata, T. Kino, G.P. Chrousos, E. Charmandari, The human glucocorticoid receptor: molecular basis of biologic function, Steroids. 75 (2010) 1–12. doi:10.1016/J.STEROIDS.2009.09.002.

[10] S. Vandevyver, L. Dejager, C. Libert, On the trail of the glucocorticoid receptor: into the nucleus and back, Traffic. 13 (2012) 364–374. doi:10.1111/J.1600-0854.2011.01288.X.

[11] W. Hofkens, G. Storm, W.B. Van Den Berg, P.L. Van Lent, Liposomal targeting of glucocorticoids to the inflamed synovium inhibits cartilage matrix destruction during murine antigen-induced arthritis, Int. J. Pharm. 416 (2011) 486–492. doi:10.1016/J.IJPHARM.2011.02.060.

[12] R. Anderson, A. Franch, M. Castell, F.J. Perez-Cano, R. Bräuer, D. Pohlers, M. Gajda, A.P. Siskos, T. Katsila, C. Tamvakopoulos, U. Rauchhaus, S. Panzner, R.W. Kinne, Liposomal encapsulation enhances and prolongs the anti-inflammatory effects of water-soluble dexamethasone phosphate in experimental adjuvant arthritis, Arthritis Res. Ther. 12 (2010). doi:10.1186/AR3089.

[13] U. Rauchhaus, F.W. Schwaiger, S. Panzner, Separating therapeutic efficacy from glucocorticoid side-effects in rodent arthritis using novel, liposomal delivery of dexamethasone phosphate: long-term suppression of arthritis facilitates interval treatment, Arthritis Res. Ther. 11 (2009). doi:10.1186/AR2889.

[14] J.M. Metselaar, M.H.M. Wauben, J.P.A. Wagenaar-Hilbers, O.C. Boerman, G. Storm, Complete remission of experimental arthritis by joint targeting of glucocorticoids with long-circulating liposomes, Arthritis Rheum. 48 (2003) 2059–2066. doi:10.1002/art.11140.

[15] Y. Mizushima, T. Hamano, K. Yokoyama, Tissue distribution and anti-inflammatory activity of corticosteroids incorporated in lipid emulsion, Ann. Rheum. Dis. 41 (1982) 263–267. doi:10.1136/ARD.41.3.263.

[16] N. Butoescu, C.A. Seemayer, M. Foti, O. Jordan, E. Doelker, Dexamethasone-containing PLGA superparamagnetic microparticles as carriers for the local treatment of arthritis, Biomaterials. 30 (2009) 1772–1780. doi:10.1016/J.BIOMATERIALS.2008.12.017.

[17] F. Yuan, L. Quan, L. Cui, S.R. Goldring, D. Wang, Development of macromolecular prodrug for rheumatoid arthritis, Adv. Drug Deliv. Rev. 64 (2012) 1205–1219. doi:https://doi.org/10.1016/j.addr.2012.03.006.

[18] G. Zhao, R. Ren, X. Wei, Z. Jia, N. Chen, Y. Sun, Z. Zhao, S.M. Lele, H.A. Zhong, M.B. Goldring, S.R. Goldring, D. Wang, Thermoresponsive polymeric dexamethasone prodrug for arthritis pain, J. Control. Release. 339 (2021) 484–497. doi:10.1016/J.JCONREL.2021.10.007.

[19] D. Funk, H.H. Schrenk, E. Frei, Development of a novel polyethylene glycol-corticosteroid-conjugate with an acid-cleavable linker, J. Drug Target. 19 (2011) 434–445. doi:10.3109/1061186X.2010.504271.

[20] S. Keely, S.M. Ryan, D.M. Haddleton, A. Limer, G. Mantovani, E.P. Murphy, S.P. Colgan, D.J. Brayden, Dexamethasone–pDMAEMA polymeric conjugates reduce inflammatory biomarkers in human intestinal epithelial monolayers, J. Control. Release. 135 (2009) 35–43. doi:10.1016/J.JCONREL.2008.12.001.

[21] M. Su, B. Yang, M. Xi, C. Qiang, Z. Yin, Therapeutic effect of pH-Responsive dexamethasone prodrug nanoparticles on acute lung injury, J. Drug Deliv. Sci. Technol. 66 (2021). doi:10.1016/J.JDDST.2021.102738.

[22] I. Dolz-Pérez, M.A. Sallam, E. Masiá, D. Morelló-Bolumar, M.D. Pérez del Caz, P. Graff, D. Abdelmonsif, S. Hedtrich, V.J. Nebot, M.J. Vicent, Polypeptide-corticosteroid conjugates as a topical treatment approach to psoriasis, J. Control. Release. 318 (2020) 210–222. doi:10.1016/J.JCONREL.2019.12.016.

[23] M. Lorscheider, N. Tsapis, M. Ur-Rehman, F. Gaudin, I. Stolfa, S. Abreu, S. Mura, P.

Chaminade, M. Espeli, E. Fattal, Mujeeb-ur-Rehman, F. Gaudin, I. Stolfa, S. Abreu, S. Mura, P. Chaminade, M. Espeli, E. Fattal, Dexamethasone palmitate nanoparticles: An efficient treatment for rheumatoid arthritis, J. Control. Release. 296 (2019) 179–189. doi:10.1016/J.JCONREL.2019.01.015.

[24] M. Lorscheider, N. Tsapis, R. Simón-Vázquez, N. Guiblin, N. Ghermani, F. Reynaud, R. Canioni, S. Abreu, P. Chaminade, E. Fattal, Nanoscale Lipophilic Prodrugs of Dexamethasone with Enhanced Pharmacokinetics, Mol. Pharm. 16 (2019) 2999–3010. doi:10.1021/acs.molpharmaceut.9b00237.

[25] L. Pinheiro do Nascimento, N. Tsapis, F. Reynaud, D. Desmaële, L. Moine, J. Vergnaud, S. Abreu, P. Chaminade, E. Fattal, Mannosylation of budesonide palmitate nanoprodrugs for improved macrophage targeting, Eur. J. Pharm. Biopharm. 170 (2022) 112–120. doi:10.1016/J.EJPB.2021.12.001.

[26] A.K. Ghosh, M. Brindisi, Organic Carbamates in Drug Design and Medicinal Chemistry, J. Med. Chem. 58 (2015) 2895–2940. doi:10.1021/JM501371S.

[27] F.M.H. De Groot, L.W.A. Van Berkom, H.W. Scheeren, Synthesis and biological evaluation of 2'-carbamate-linked and 2'-carbonate-linked prodrugs of paclitaxel: selective activation by the tumor-associated protease plasmin, J. Med. Chem. 43 (2000) 3093–3102. doi:10.1021/JM0009078.

[28] R. Canioni, F. Reynaud, T. Leite-Nascimento, C. Gueutin, N. Guiblin, N.E. Ghermani, C. Jayat, P. Daull, J.S. Garrigue, E. Fattal, N. Tsapis, Tiny dexamethasone palmitate nanoparticles for intravitreal injection: Optimization and in vivo evaluation, Int. J. Pharm. 600 (2021). doi:10.1016/j.ijpharm.2021.120509.

[29] T. Mosmann, Rapid colorimetric assay for cellular growth and survival: application to proliferation and cytotoxicity assays, J. Immunol. Methods. 65 (1983) 55–63. doi:10.1016/0022-1759(83)90303-4.

[30] D.G. Altman, M.F.W. Festing, Guidelines for the Design and Statistical Analysis of Experiments Using Laboratory Animals, ILAR J. 43 (2002) 244–258. doi:10.1093/ilar.43.4.244.

[31] L. Quan, Y. Zhang, B.J. Crielaard, A. Dusad, S.M. Lele, C.J.F. Rijcken, J.M. Metselaar, H. Kostková, T. Etrych, K. Ulbrich, F. Kiessling, T.R. Mikuls, W.E. Hennink, G. Storm, T. Lammers, D. Wang, Nanomedicines for inflammatory arthritis: head-to-head comparison of glucocorticoid-containing polymers, micelles, and liposomes., ACS Nano. 8 (2014) 458–466. doi:10.1021/nn4048205.

[32] T. Yardeni, M. Eckhaus, H.D. Morris, M. Huizing, S. Hoogstraten-Miller, Retro-orbital injections in mice, Lab Anim. (NY). 40 (2011) 155–160. doi:10.1038/LABAN0511-155.

[33] R. Simón-Vázquez, N. Tsapis, M. Lorscheider, A. Rodríguez, P. Calleja, L. Mousnier, E. de Miguel Villegas, Á. González-Fernández, E. Fattal, Improving dexamethasone drug loading and efficacy in treating arthritis through a lipophilic prodrug entrapped into PLGA-PEG nanoparticles, Drug Deliv. Transl. Res. 12 (2022) 1270–1284. doi:10.1007/S13346-021-01112-3/FIGURES/8.

[34] B. Tessier, N. Tsapis, E. Fattal, L. Moine, Emerging nanoparticle platforms to improve the administration of glucocorticoids, J. Control. Release. 358 (2023) 273–292. doi:10.1016/J.JCONREL.2023.04.039.

[35] International Standard Organization, ISO 10993-5 - Part 5: Tests for in vitro cytotoxicity, 2009.

[36] A.J.M. D'Souza, E.M. Topp, Release from polymeric prodrugs: linkages and their degradation, J. Pharm. Sci. 93 (2004) 1962–1979. doi:10.1002/JPS.20096.

[37] A. Bordat, T. Boissenot, N. Ibrahim, M. Ferrere, M. Levêque, L. Potiron, S. Denis, S. Garcia-Argote, O. Carvalho, J. Abadie, C. Cailleau, G. Pieters, N. Tsapis, J. Nicolas, A Polymer Prodrug Strategy to Switch from Intravenous to Subcutaneous Cancer Therapy for Irritant/Vesicant Drugs, J. Am. Chem. Soc. 144 (2022) 18844–18860. doi:10.1021/JACS.2C04944/SUPPL_FILE/JA2C04944_SI_001.PDF.

[38] B. Matter, A. Ghaffari, D. Bourne, Y. Wang, S. Choi, U.B. Kompella, Dexamethasone Degradation in Aqueous Medium and Implications for Correction of In Vitro Release from Sustained Release Delivery Systems, AAPS PharmSciTech. 20 (2019). doi:10.1208/S12249-019-1508-7.

[39] E.J. Begg, H.C. Atkinson, N. Gianarakis, The pharmacokinetics of corticosteroid agents, Med. J. Aust. 146 (1987) 37–41. doi:10.5694/J.1326-5377.1987.TB120124.X.

[40] M.T. Peracchia, E. Fattal, D. Desmaële, M. Besnard, J.P. Noël, J.M. Gomis, M. Appel, J. D'Angelo, P. Couvreur, Stealth(®) PEGylated polycyanoacrylate nanoparticles for intravenous administration and splenic targeting, J. Control. Release. 60 (1999) 121–128. doi:10.1016/S0168-3659(99)00063-2.

[41] S. Zalba, T.L.M. ten Hagen, C. Burgui, M.J. Garrido, Stealth nanoparticles in oncology: Facing the PEG dilemma, J. Control. Release. 351 (2022) 22–36. doi:10.1016/J.JCONREL.2022.09.002.